Electronic Supplementary Material (ESI) for Physical Chemistry Chemical Physics.

Table S1. The stepwise and average pK_a values of the His19 and His27 tetrad are obtained by Toyama[a], Hong Mei[b] and Wang Jun[c] in various lipid membranes.

	the His19 tetrad			the His27 tetrad	
	Toyama's	Hong Mei's	Wang Jun's	Toyama's	Hong Mei's
pK_a1	-	6.1	-	-	7.9
pK_a2	-	5.7	-	-	5.9
pK_a3	-	4.5	4.49	-	5.9
pK_a4	-	4.2	3.10	-	5.8
av pK_a	6.5	5.1	-	7.6	6.4

[a] Data from Journal of biochemistry 2009, 145, 543-554.

[b] Data from Journal of the American Chemical Society 2016, 138, 8143-8155.

[c] Data from Biochemistry 2009, 48, 9949-9951.

Table S2. $BM2_{TM}$ models for classic fixed-protonation-state MD simulations, which are the coupling between 6 charge states ($His19^{0}_{4}$, $His19^{1+}_{4}$, $His19^{2a+}_{4}$, $His19^{2d+}_{4}$, $His19^{3+}_{4}$, $His19^{4+}_{4}$) of the His19 tetrad and 2 states of the His27 tetrad (neutral state $His27^{0}_{4}$ or full-cationic state $His27^{4+}_{4}$).

His19 / His27	$His19^{0}_{4}$	$His19^{1+}_{4}$	$His19^{2a+}_{4}$	$His19^{2d+}_{4}$	$His19^{3+}_{4}$	$His19^{4+}_{4}$
neutral state $His27^{0}_{4}$	100 ns	100 ns	100 ns	100 ns	100 ns	100 ns
full-cationic state $His27^{4+}_{4}$	100 ns	100 ns	100 ns	100 ns	100 ns	100 ns

Table S3. The QM/MM models of the neutral ($His27^{0}_{4}$) and full-cationic ($His27^{4+}_{4}$) systems

system	neutral ($His27^{0}_{4}$) systems			full-cationic ($His27^{4+}_{4}$) systems		
The state of the His19 tetrad	Q1	Q2	Q3	Q1	Q2	Q3
QM model	Four His19 and three water molecules	Four His19 and four water molecules	Four His19 and five water molecules	Four His19 and two water molecules	Four His19 and Five water molecules	Four His19 and six water molecules
The atomic numbers of QM model	54	58	62	51	61	65
Total atomic numbers	34385	34386	34387	34381	34382	34383
Total simulation time(ns)	32.5	32.5	32.5	32.5	32.5	32.5

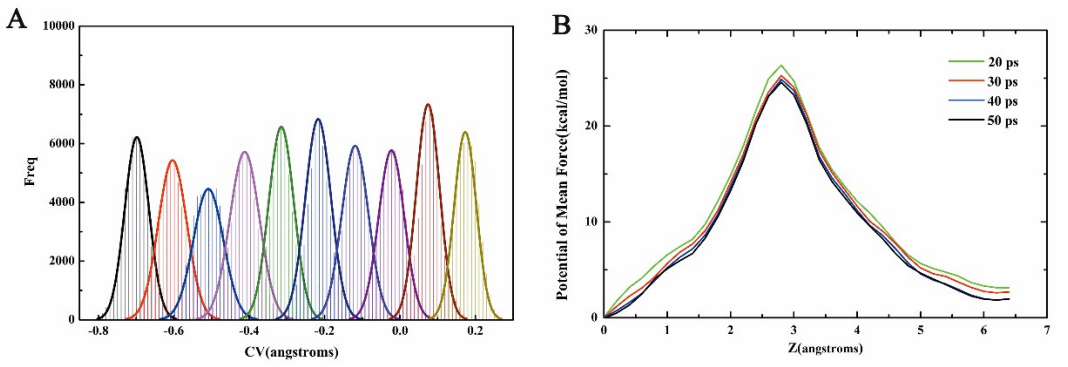

Fig. S1 (A) The overlap between the simulation windows for the Q1 state channel in full-cationic ($^{His27^{4+}}_{4}$) systems. (B) Convergence of the PMFs calculated by umbrella sampling, where 50 ps US simulations were performed for the Q1 state channel in full-cationic ($^{His27^{4+}}_{4}$) systems. PMFs are shown with the simulation time of 20, 30, 40, and 50 ps, respectively.

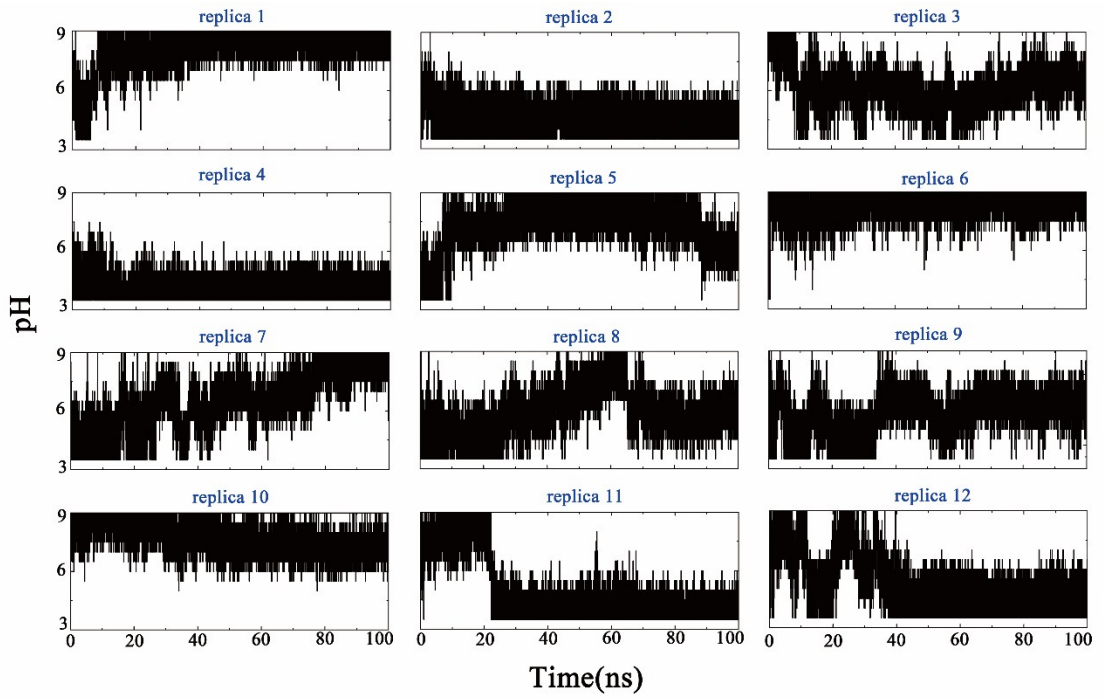

Fig. S2 Replica walk in the pH space as a function of simulation time for 12 pH replicas.

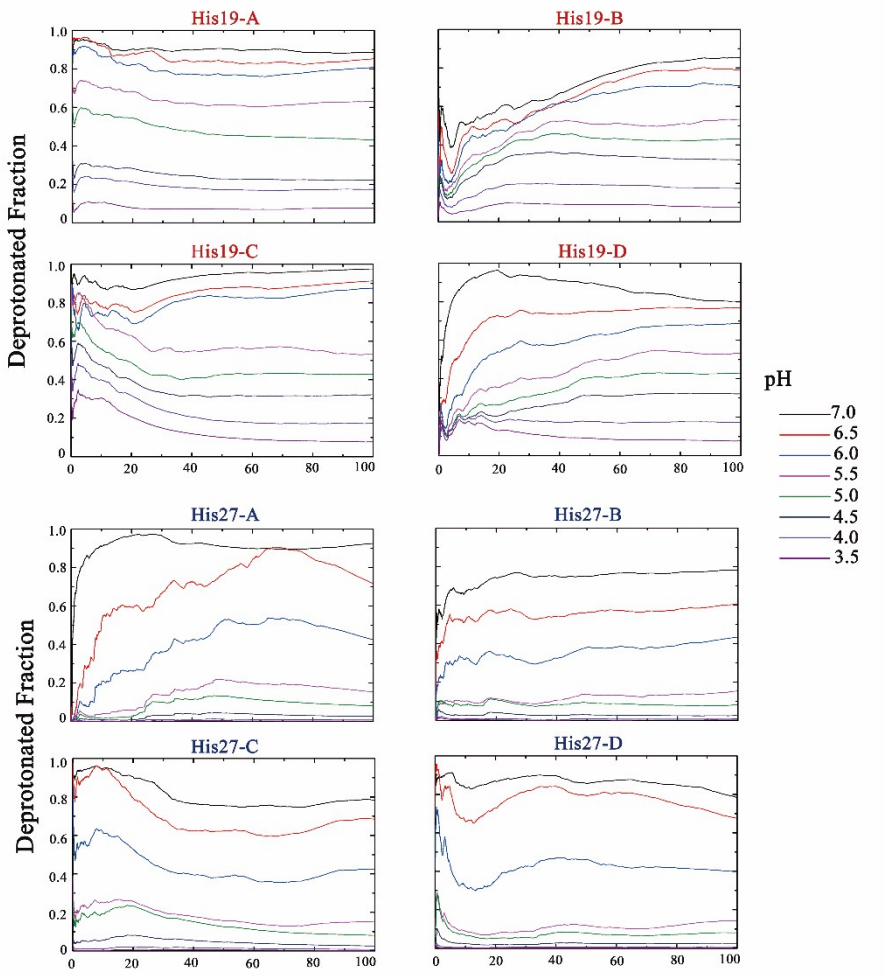

Fig. S3 The deprotonated fraction of His19 and His27 tetrad as a function of simulation time.

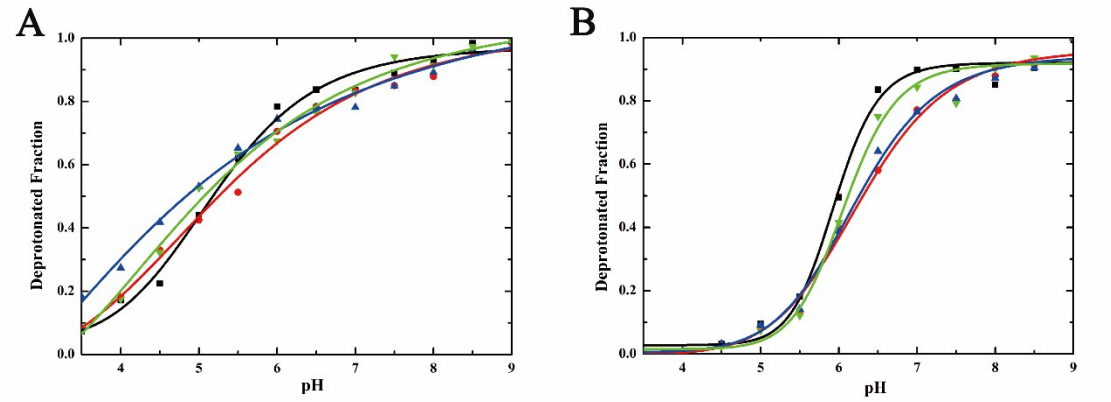

Fig. S4 Microscopic titration of His19 and His27. (A) Deprotonated fraction of individual His19 residues at different pH, and four microscopic pK_a's: 4.97, 5.19, 5.23, and 5.35. (B) Deprotonated fraction of individual His17 residues at different pH, and and four microscopic pK_a's: 6.00, 6.18, 6.33, and 6.37. Four colors represent four residues.

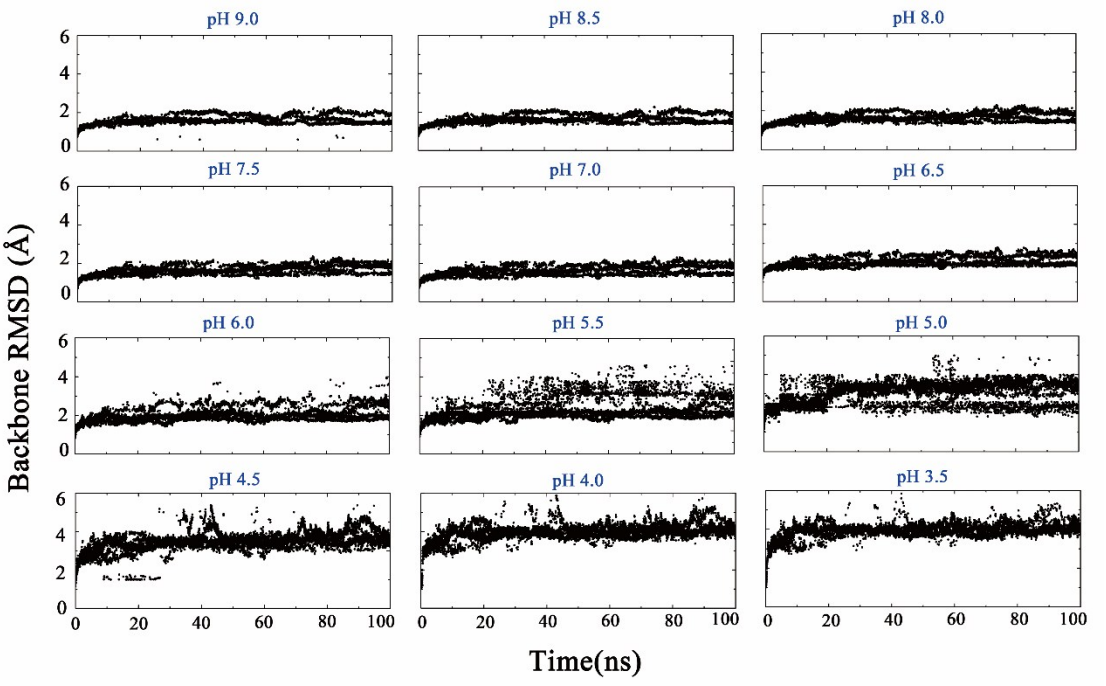

Fig. S5 The backbone RMSD with respect to the equilibrium structure as a function of simulation time under simulated pH conditions.

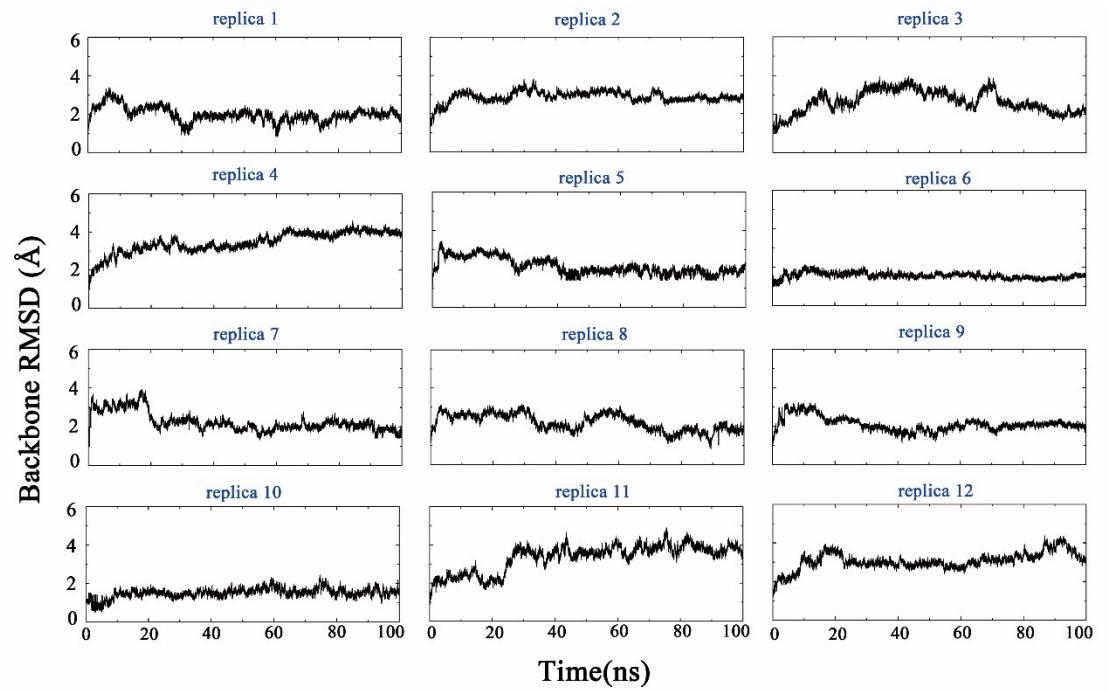

Fig. S6 The backbone RMSD with respect to the equilibrium structure as a function of simulation time for all replicas.

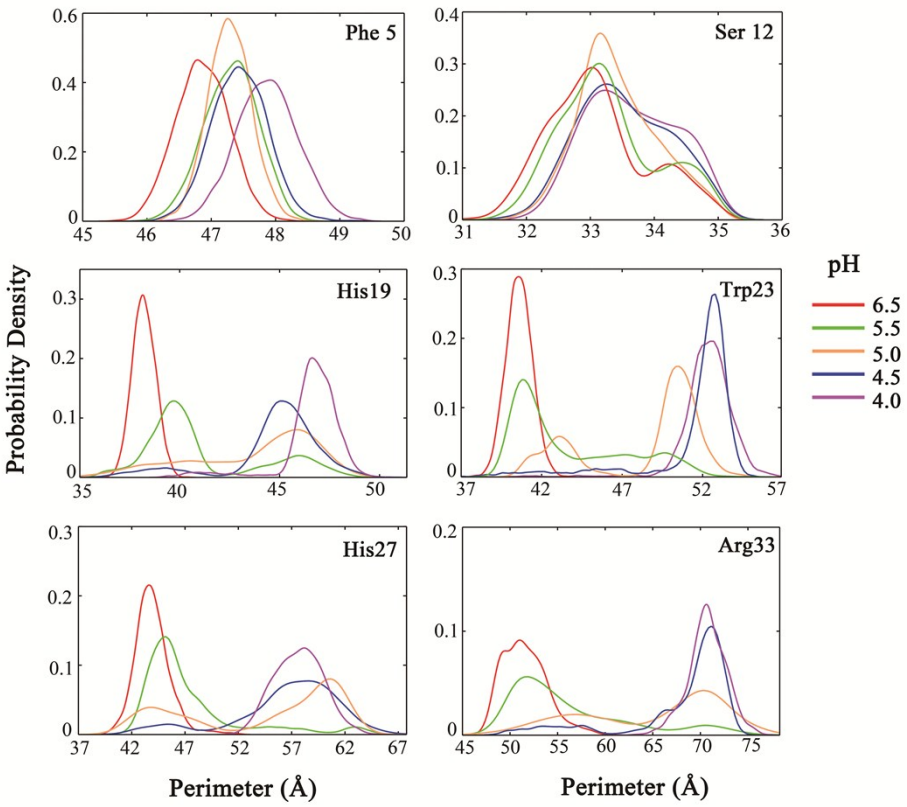

Fig. S7 Probability distribution of perimeters at different locations along the pore of BM2 under different pH conditions.

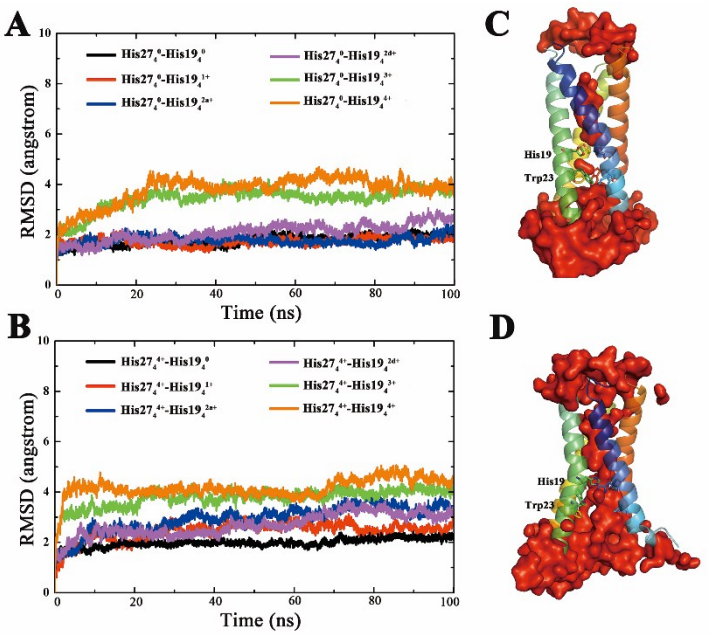

Fig. S8 The RMSD values of the protein backbone atoms with respect to the initial frame of the production step as a function of simulation time. (A) The RMSD values when the His19 tetrad is at 0, +1, +2a (adjacent position), +2d (diagonal position), +3 and +4 charge state in the $His27^{0}_{4}$ systems. (B) The RMSD values in the $His27^{4+}_{4}$ systems. (C) The distribution of water density for closed state calculated from the simulation is shown as red shading. (D) The distribution of water density for open state.